PFC/JA-85-23R

A ONE-DIMENSIONAL MODEL FOR LOWER HYBRID
CURRENT DRIVE INCLUDING PERPENDICULAR DYNAMICS**

V. Fuchs*, R. A. Cairns*+, M. M. Shoucri*

K. Hizanidis and A. Bers

Revised
September 1985

Plasma Fusion Center
Massachusetts Institute of Technology
Cambridge, Massachusetts 02139 USA

A ONE-DIMENSIONAL MODEL FOR LOWER HYBRID CURRENT DRIVE INCLUDING PERPENDICULAR DYNAMICS

V. Fuchs, R. A. Cairns[a], and M. M. Shoucri
Projet Tokamak, Institut de Recherche d'Hydro-Québec
Varennes, Québec, Canada JOL 2PO

K. Hizanidis and A. Bers
Plasma Fusion Center, Massachusetts Institute of Technology
Cambridge, Massachusetts 02139, USA

The 2-D (velocity space) Fokker-Planck equation for lower-hybrid current drive is approximated by its perpendicular moments hierarchy closed in the second moment equation. The closure is derived on the basis of a distribution function composed of a central thermal Maxwellian plus a perpendicularly broadened distribution of fast particles that are diffused into, and pitch-angle scattered out of, the quasilinear plateau region. The resulting 1-D model reproduces the relevant features of the solutions obtained from numerically integrating the 2-D Fokker-Planck equation. An analytic estimate of the perpendicular temperature on the plateau and the plateau height as a function of spectrum width and position is presented. Also predicted are the current density generated and its figure of merit (the current density per unit power density dissipated).

[a]Permanent address: University of St. Andrews, St. Andrews, KY169SS, Scotland

I. INTRODUCTION

This paper presents a new one-dimensional (1-D, velocity space, parallel to the magnetic field $\vec{B}_0$) theory for lower-hybrid (LH) current drive with proper account of the essential perpendicular (to $\vec{B}_0$) dynamics. The purpose of this work is to obtain a simple model which correctly predicts the essential features of LH current drive that are now obtainable only from 2-D numerical integrations of the Fokker-Planck equation. The conventional 1-D treatment[1] assumes a Maxwellian distribution at bulk temperature in the perpendicular direction for all parallel velocities. However, numerical integrations of the 2-D Fokker-Planck equation with quasilinear diffusion show that the pitch-angle scattering of particles leads to a perpendicular temperature in the plateau region that is significantly enhanced over the bulk temperature[2]. Further, these calculations also show that the height of the quasilinear plateau is also enhanced over that given by 1-D theory thus giving a higher current. In addition, experiments in LH current drive have clearly shown that the perpendicular distribution function has characteristic energies one-to-two orders of magnitude larger than the bulk temperature. For these reasons the simple one-dimensional Fokker-Planck model does not give satisfactory results. We reconsider here a model[3] in which we take into account two moments of the distribution with respect to the perpendicular velocity, namely $F(v_{\parallel}) = 2\pi \int_0^{\infty} v_{\perp} f(v_{\perp}, v_{\parallel}) dv_{\perp}$ and $F_2(v_{\parallel}) = 2\pi \int_0^{\infty} v_{\perp}^3 f dv_{\perp}$. When moments of the Fokker-Planck equation are taken, the equation for F_2 involves the higher moment $\int_0^{\infty} v_{\perp}^5 f dv_{\perp}$, and some closure assumption is necessary.

From the 2-D numerical results it is clear that the effect of the rf spectrum is not confined to the region of $v_{\parallel}$ in which it falls, but that high energy particles are pitch-angle scattered back to lower $v_{\parallel}$. At values of $v_{\parallel}$ below the plateau the distribution may be expected to consist of a central Maxwellian plus a tail of fast particles originating in the

plateau. For such a distribution the closure assumption $< v_\perp^4 > = 2 < v_\perp^2 >^2$, which is exact for a Maxwellian, is not likely to be very accurate. The essential new step in our theory is to recognize this, and to write the distribution function as $f = f_M + \tilde{f}$, with f_M the bulk Maxwellian, then deal with moments of $\tilde{f}$ and apply the closure assumption to them. Numerical solutions of the resulting one-dimensional equations indicate that they are capable of accurately reproducing the main features of the 2-D solutions, namely $F(v_\parallel)$ and $T_\perp(v_\parallel) = F_2/2F$. An independent estimate of the plateau temperature based on the slowing down equations allows a simplification of the equations to the extent that it permits analytic estimates of the plateau height and slope (and therefore also of the rf current and power dissipated) as a function of spectrum width and position.

An important advantage of our predictive 1-D model is that it is enormously simpler to evaluate than the numerical integration of the full 2-D equations and hence can be readily coupled to existing transport codes. In this manner one should be able to achieve a more complete description of LH current drive which includes the effects of plasma profiles and transport. This, however, is beyond the scope of this paper.

In Sec. II we present the Fokker-Planck equation and 2-D numerical results pertinent to the understanding of the behavior of the fast particles. In Sec. III we present the perpendicular moment equations and the closure assumption. In Sec. IV we derive the plateau temperature and boundary conditions, and in Sec. V we present numerical results based upon our new 1-D model and our conclusions. Details of the perpendicular velocity averaging of the Fokker-Planck equation are presented in the Appendix.

II. THE DISTRIBUTION FUNCTION FROM 2-D NUMERICAL INTEGRATION OF THE FOKKER-PLANCK EQUATION

During lower-hybrid current drive the departure of the electron distribution function f from a Maxwellian equilibrium f_M,

$$f_M = (2\pi)^{-3/2} \exp(-v^2/2)\,, \qquad (1)$$

where we normalized v to thermal velocity, v_e, i.e. $v \to v/v_e$, $v_e^2 = kT/m_e$, is caused by fast electrons continuously diffused into, and pitch-angle scattered out of, the rf-generated quasilinear plateau. The characteristic features of the fast electron population can be readily seen and understood from numerical solutions of the steady-state 2-D Fokker-Planck equation

$$\mathrm{div}\ \vec{S} \equiv \frac{1}{v_\perp}\frac{\partial}{\partial v_\perp}(v_\perp S_\perp) + \frac{\partial S_\parallel}{\partial v_\parallel} = 0\,, \qquad (2)$$

where the test-particle flux

$$\vec{S} = -\overleftrightarrow{D}\cdot\ \mathrm{grad}\ f + \vec{S}_{\mathrm{coll}}, \qquad (3)$$

is defined in the coordinate system v_x, v_y, v_z where direction z corresponds to the externally applied magnetic field; to simplify notation we also let $z \equiv v_\parallel = v_z$, $v_\perp^2 = v_x^2 + v_y^2$. $\vec{S}$ has contributions from the quasilinear diffusion tensor $\overleftrightarrow{D} = \overleftrightarrow{D}_{QL}/\nu_0 v_e^2$, where $\nu_0 = 4\pi n_e e^4 \ln \Lambda / m_e^2 v_e^3$ (recalling that for lower-hybrid waves only the parallel component $D_{zz} \equiv D$ is significant), and from collisions with the field ions and electrons. Explicitly, linearizing the collisional operator for $v \gg 1$,

$$S_\parallel = -D\frac{\partial f}{\partial z} - \frac{A}{2}\frac{v_\perp^2}{v^4}\frac{\partial f}{\partial \mu} - B\frac{z}{v^4}\left(vf + \frac{\partial f}{\partial v}\right), \qquad (4)$$

$$S_\perp = \frac{A}{2v^4}zv_\perp\frac{\partial f}{\partial \mu} - B\frac{v_\perp}{v^4}\left(vf + \frac{\partial f}{\partial v}\right), \qquad (5)$$

where $\mu = z/v$, and the collisional flux is taken in the approximation of Maxwellian field ions and electrons with $T_e = T_i$. In the 2-D code[4] we use the most general expressions for the coefficients $A(v)$ and $B(v)$[5], but otherwise we work with their simpler high-energy limits

$$A \simeq 1 + Z_i\,, \quad B \simeq 1 \qquad (6)$$

4

which leave the bulk unmodified.

In the subsequent analysis, we make extensive use of the perpendicular velocity moments F_n of the distribution function f defined as

$$F_n(z) = 2\pi \int_0^\infty v_\perp^{n+1} f(z, v_\perp) \, dv_\perp \quad ; \quad n = 0, 2, 4 \,. \tag{7}$$

In terms of these moments F_n, we further define the "parallel" distribution $F(z)$ and the "perpendicular" temperature $T_\perp(z)$

$$F(z) = F_0 \quad , \quad T_\perp(z) = F_2/2F_0 \,. \tag{8}$$

For a Maxwellian (1) we have

$$F_{0M} = (2\pi)^{-1/2} \exp(-z^2/2) \,, \quad F_{2M} = 2F_M \,, \quad T_\perp = 1 \,. \tag{9}$$

A numerical integration of the Fokker-Planck equation (2) with (4) and (5) gives the steady-state distribution function $f(z, v_\perp)$ for a given $D(z)$. From this one can then obtain (also numerically) the parallel distribution function and perpendicular temperature as defined in (8). A typical result for an rf field of practical interest (i.e. $D > 1$), with a spectrum lying within the bounds $v_1 \le z \le v_2$, is shown in Fig. 1. The parallel distribution function F is seen to consist of three distinct parts. The thermal bulk, the quasilinear plateau, and a tail of hot particles pitch-angle scattered out of the plateau. The pitch-angle scattering of fast particles out of the plateau is evident from the flux vector plot of Fig. 2. Returning to Fig. 1, we note that the perpendicular temperature $T_\perp$ is, in fact, a signature of the fast particles, the broadening in the perpendicular direction resulting from an influx of particles (into the resonant region) at low $v_\perp$ and their collisional scattering to larger $v_\perp$ inside the resonant region. The height of the plateau exceeds the Maxwellian value $F_M(v_1)$ by about a factor of 3, the enhancement obviously resulting from the larger number of particles associated with the enhanced $T_\perp$ there. We can therefore expect the plateau height to increase with increasing perpendicular

temperature on the plateau, which in turn depends on the spectrum width and position. This is illustrated in Table I.

Further evidence of the fast particles can be found in Fig. 3. Plotted there are moments of $\tilde{f} = f - f_M$. Thus $\tilde{F}_0$ signifies the non-Maxwellian part of the distribution. The perpendicular temperature of this population is $\tilde{F}_2/2\tilde{F}_0$. It can be seen that this, which is clearly due to particles with high perpendicular velocities, is large and essentially independent of $v_{\parallel}$. The moment $\tilde{F}_4$ again confirms this since higher order moments are increasingly dominated by fast particles. Finally, Fig. 4 depicts perpendicular cuts through the distribution function f at 6 different positions of z. The broadened character of these cuts inside the resonant region gives a measure of the particles that enhance the plateau value of F_0. Above and on the plateau, f is dominated by the fast particles, but near the lower bound of the plateau we see emerging the thermal core, which will rapidly dominate the fast population as z is further decreased. The rapid increase of $T_{\perp}$ just below the plateau seen in Fig. 1 is now easily explained in general terms by the fact that the thermal bulk Maxwellian increases rapidly in magnitude as z is reduced below the lower bound of the plateau. More specifically, if we represent $\tilde{f}$ by

$$\tilde{f} = \frac{\tilde{F}(z)}{2\pi\tilde{T}(z)} \exp[-v_{\perp}^2/2\tilde{T}(z)], \tag{10}$$

where $\tilde{T}$ is the perpendicular temperature of the fast population, we get

$$T_{\perp}(z) = \frac{F_2}{2F_0} = \frac{F_M + \tilde{T}\tilde{F}}{F_M + \tilde{F}}, \tag{11}$$

yielding $T_{\perp} = \tilde{T}$ on the plateau, and $T_{\perp} = 1$ below, with the transition occurring in the region where $F_M \simeq \tilde{F}$.

From the numerical integration of the 2-D Fokker-Planck model (2)–(5) we reach the following conclusions. Fast particles generated by a wide lower-hybrid spectrum strongly

modify the distribution function via perpendicular dynamics. The two principal features are an enhanced quasilinear plateau and a strongly enhanced perpendicular temperature in the plateau. Conventional 1-D theories based on the averaged Fokker-Planck equation cannot self-consistently yield these effects since the shape of the distribution function in the perpendicular direction must be specified in advance. In the next section we will attempt a self-consistent 1-D treatment by taking two moments of the Fokker-Planck equation.

III. PERPENDICULAR MOMENT EQUATIONS

The results of the preceding section indicate that the distribution function can be conveniently represented in the form

$$f = f_M + \tilde{f} , \tag{12}$$

where $\tilde{f}$ is the distribution of fast particles, approximately given by (10). This function depends on two unknown functions $\tilde{F}(z)$ and $\tilde{T}(z)$, so that we need to take at least two moments of the Fokker-Planck equation (2) in order to be able to determine these unknown functions. We will shortly see that just two moments are needed, since the hierarchy progresses through even orders.

To begin, let us take the $n = 0$ perpendicular velocity moment of Eq. (2). The integral of $S_\perp$ vanishes, so that we have

$$dS_0/dz = 0 , \tag{13}$$

where we define

$$S_n = 2\pi \int_0^\infty v_\perp^{n+1} S_\| \, dv_\perp , \ n = 0, 2, \ldots , \tag{14}$$

with $S_\|$ given by (4) in which we substitute

$$\frac{\partial f}{\partial \mu} = v\left(\frac{\partial f}{\partial z} - \frac{z}{v_\perp} \frac{\partial f}{\partial v_\perp} \right) \tag{15a}$$

7

and

$$\frac{\partial f}{\partial v} = \frac{1}{v}\left(z\frac{\partial f}{\partial z} + v_\perp \frac{\partial f}{\partial v_\perp}\right). \qquad (15b)$$

The integrals arising in (14) are evaluated in the Appendix. The model presented in this section is based upon a simple approximation of these integrals, obtained by replacing everywhere in $S_\parallel$ the particle velocity v by $v_\parallel \equiv z$, and neglecting terms $O(1/z^4)$ and higher. This model is valid for particles having $z \gg v_\perp$, and in regions of $v_\parallel$ where $z^2 \gg 2T_\perp$. Thus, in this simple approximation, we obtain

$$S_0 = -\frac{A+B}{z^2}F - \left(D + \frac{B}{z^3}\right)F' - \frac{A}{2z^3}F_2', \qquad (16)$$

where the prime stands for d/dz. The flux S_0 contains the additional unknown F_2, so that we need to take the next ($n=2$) moment of (2) which gives

$$\frac{\partial S_2}{\partial z} - 4\pi \int_0^\infty v_\perp^2 S_\perp \, dv_\perp = 0. \qquad (17)$$

Using (4)–(7), we then find

$$4\pi \int_0^\infty v_\perp^2 S_\perp \, dv_\perp = \frac{2AF}{z} + \frac{AF_2'}{z^2} - \frac{2BF_2}{z^3} \qquad (18)$$

and

$$S_2 = -\frac{2A+B}{z^2}F_2 - \left(D + \frac{B}{z^3}\right)F_2' - \frac{A}{2z^3}F_4', \qquad (19)$$

where we have likewise neglected terms $O(1/z^4)$ and higher. Equation (19) contains the further unknown F_4, so that the system is still not closed. We therefore have to either continue the hierarchy in the anticipation that the higher-order moments are less and less important, or we close the hierarchy at the given second level. The first alternative does not seem feasible since the higher-order moments of the distribution function are more and more dominated by the fast particles and are therefore larger and larger. Moreover, this approach would not serve the original purpose of this work which is to produce a

8

sufficiently accurate but simple model. We therefore adopt the second alternative, which is to find a closure. Here we have two choices. The first would be to make an assumption about the form of f in terms of *two* trial functions [i.e. $\tilde{F}$ and $\tilde{T}$ if we adopt the form of f defined by Eqs. (10) and (12)] and express F_0, F_2 and F_4 in terms of these. The second is to seek to express F_4 in terms of F_2 directly, given some clue about the behavior of the moments F_n as their order increases.

It proves convenient to set $f = f_M + \tilde{f}$, and write the moment equations in terms of $\tilde{F}_n$, whose dependence on z (Fig. 3) does not have the rapid, boundary-layer-type, behavior exhibited by $T_\perp$ in Fig. 1. The collisional flux annihilates the Maxwellian f_M so that the moment equations become

$$\frac{d}{dz}\left[-\frac{A+1}{z^2}\tilde{F} - \left(D + \frac{1}{z^3}\right)\tilde{F}' - \frac{A}{2z^3}\tilde{F}'_2 + zDF_M \right] = 0 \tag{20}$$

and

$$\frac{d}{dz}\left[-\frac{3A+1}{z^2}\tilde{F}_2 - \left(D + \frac{1}{z^3}\right)\tilde{F}'_2 - \frac{A}{2z^3}\tilde{F}'_4 + 2zDF_M \right] = \frac{2A\tilde{F}}{z} + \frac{2(A-B)\tilde{F}_2}{z^3} \tag{21}$$

If for $\tilde{f}$ we now adopt the plausible form (10), we have $\tilde{F}_2 = 2\tilde{T}\tilde{F}$ and

$$\tilde{F}_4 = 2\pi \int_0^\infty v_\perp^5 \tilde{f}\, dv_\perp = 4\tilde{T}\tilde{F}_2 = 4\tilde{F}_2^2/\tilde{F}\,, \tag{22}$$

whereupon (20) and (21) become a nonlinear system for $\tilde{F}_0$ and $\tilde{F}_2$. Then, by definition, $F = F_M + \tilde{F}$, and $T_\perp$ is given by (11).

We are, however, not obliged to restrict ourselves to the perpendicular Maxwellian (10). As a matter of fact, a simpler system is obtained if we recognize that the fast particles initially scattered out of the plateau at the plateau temperature T_p remain at $\tilde{T} \simeq T_p$ as was described in relation to Fig. 3. This means that $\tilde{F}_2/\tilde{F}$ remains fairly constant, and this must hold even more for $\tilde{F}_4/\tilde{F}_2$, since the higher order moments are increasingly dominated by the fast particles. We can thus safely use the closure

$$\tilde{F}_4 = C_4 T_p \tilde{F}_2 . \tag{23}$$

This procedure gives a *linear* system but, of course, requires an independent estimate of the plateau temperature T_p. Then C_4 is just a normalization constant which, on the basis of the Maxwellian result (22), can be set equal to 4.

An even simpler procedure would be to take the lower order closure

$$\tilde{F}_2 = C_2 T_p \tilde{F} , \tag{24}$$

which again requires an estimate of T_p, and where C_2 can be taken as 2. This, lowest order, approximation still gives quite good results, as we shall see in Sec. V., and moreover can be treated analytically.

In order to solve Eqs. (20) and (21) we need four boundary conditions, and an independent estimate of the plateau temperature. We will deal with these questions in the next section.

IV. BOUNDARY CONDITIONS AND PLATEAU TEMPERATURE

Let us first discuss the boundary conditions for Eqs. (20) and (21). Equation (20) can be immediately integrated once. The integration constant is determined by the condition of zero net particle flux, $S_0 = 0$. Three other boundary conditions now need to be considered. We will show that in order to avoid an ill-posed problem, just one condition is to be applied in the region of large z (above the plateau), while the remaining two are applied at the lower bound of integration (below the plateau). In order to show this and to formulate the large-z boundary condition, we will consider the asymptotic solutions of Eqs. (20) and (21).

For this purpose we use the closure (23) which linearizes the system, and we assume WKB solutions

$$\tilde{F}_1, \tilde{F}_2 \sim \exp[\int \lambda(z)\, dz] . \tag{25}$$

10

This leads to a characteristic equation

$$\lambda\left\{-\frac{A^2}{z} + [\lambda + (A+1)T_p]\left[\frac{3A+1}{z^2} + \frac{\lambda}{z^3}(1 + 2AT_p)\right]\right\} = 0 \,. \tag{26}$$

The root $\lambda = 0$ is inadmissible, the other two (for $Z_i = 1$) are

$$\left(\frac{\lambda}{z}\right)_{1,2} \equiv a_{1,2} = \frac{1}{1+4T_p}\left\{-6T_p - 5 \pm [(6T_p + 5)^2 - 17(1 + 4T_p)]^{1/2}\right\} \tag{27}$$

where the discriminant is positive-definite. Both roots are negative but $|a_1| \ll |a_2|$, so that for large z the solution is dominated by the root a_1, i.e.

$$\tilde{F}_1, \tilde{F}_2 \sim (a_1 z^2/2) \,. \tag{28}$$

This yields for large z a condition of the mixed type for the flux S_2, (19),

$$S_2 + \tilde{F}_2(2A + 1 + a_1 + 2Aa_1 T_p)/z^2 = 0 \,. \tag{29}$$

Below the plateau, pitch-angle scattering is stronger ($\sim v^{-3}$), so that throughout the bulk $\tilde{F}$ remains large, at about the plateau height F_p, with a plateau temperature T_p. The boundary conditions in the bulk hence are

$$\tilde{F} \simeq F_p \,, \quad \tilde{F}_2 \simeq 2T_p F_p \,. \tag{30}$$

In order to implement these conditions, together with the closure (23) or (24), we need an estimate of the plateau temperature T_p. This can be obtained using the slowing down equations. We know that with an rf-field the plateau is produced by strong diffusion of the particles in z within the rf-range $v_1 \leq z \leq v_2$. Superimposed on the rf diffusion there is the collisional slowing down of the particles. We shall suppose that the average time spent in the plateau region is determined by the collisional slowing down. The picture is of a systematic slowing down of the particle on the collisional time scale on which is superimposed a fast random motion in z (due to the large RF diffusion) while the particle is in the plateau region. The (normalized) momentum and energy slowing down equations are[6]

11

$$\frac{dz}{dt} = -(2 + Z_i)\frac{z}{v^3} \qquad (31)$$

$$\frac{dv}{dt} = -\frac{1}{v^2} , \qquad (32)$$

giving

$$\frac{dv}{dz} = \frac{v}{(2 + Z_i)z} , \qquad (33)$$

or

$$v = v_0(z/z_0)^{\frac{1}{2+Z_i}} , \qquad (34)$$

so that

$$v_\perp^2 = v^2 - z^2 = v_0^2(z/z_0)^{\frac{2}{2+Z_i}} - z^2 , \qquad (35)$$

where z_0 and v_0 are initial values. This gives the average perpendicular energy acquired as a result of pitch-angle scattering of the particle as z decreases from z_0 to z.

Now, for strong rf diffusion, particles taken from the bulk are spread more or less uniformly over the plateau region. Suppose that the average time taken by them to escape from this region is determined by their collisional slowing down, so that in using (35) we are interested in the perpendicular energy acquired by a particle with $z = v_1$, the lower end of the plateau and z_0 (the initial $v_\parallel$) distributed with equal probability over the region $v_1 \leq z \leq v_2$. We therefore take $z = v_1$ in Eq. (35), and suppose that the distribution of particles in $v_\perp$ corresponds to a uniform distribution of z_0 over (v_1, v_2). Then on the plateau

$$< v_\perp^2 >_p = \frac{1}{v_2 - v_1} \int_{v_1}^{v_2} v_\perp^2 \, dz_0 \equiv 2T_p \qquad (36)$$

giving

$$T_p = \frac{v_1^{2-\alpha_i}}{2(v_2 - v_1)}\left(\frac{v_2^{\alpha_i+1} - v_1^{\alpha_i+1}}{\alpha_i + 1} + v_{\perp 0}^2\frac{v_2^{\alpha_i-1} - v_1^{\alpha_i-1}}{\alpha_i - 1}\right) - \frac{v_1^2}{2} , \qquad (37)$$

12

where $\alpha_i = (2 + 2Z_i)/(2 + Z_i)$ and $v_{\perp 0}^2$ is the initial spread in $v_\perp$. A lower bound for T_p is immediately obtained by ignoring $v_{\perp 0}^2$ (or taking $v_{\perp 0}^2 = 2$, the bulk value). To get an upper bound we take $v_{\perp 0}^2 \simeq T_p$, i.e. a mean between the bulk and the plateau. We thus get

$$T_p^{(\min)} = \frac{3}{14}v_1^{2/3}\frac{v_2^{7/3} - v_1^{7/3}}{v_2 - v_1} - \frac{v_1^2}{2} \tag{38a}$$

$$T_p^{(\max)} = \frac{\frac{1}{7}(v_2^{7/3} - v_1^{7/3}) - \frac{1}{3}(v_2 - v_1)v_1^{4/3}}{\frac{2}{3}(v_2 - v_1)v_1^{-2/3} - v_2^{1/3} + v_1^{1/3}} . \tag{38b}$$

A few cases of T_p thus calculated are shown in Table II. In all of the cases, the numerically obtained T_p from 2-D results lie, as expected, in-between the two limits and closer to $T_p^{(\max)}$.

We are finally in a position to integrate Eqs. (20) and (21) and make a comparison with the 2-D results. This will be done in the next section.

V. RESULTS AND DISCUSSION

In order to test our 1-D formalism, we will numerically integrate Eqs. (20) and (21) for parameters corresponding to the 2-D results of Sec. II, i.e. for $D = 3$ in the range $4 \leq z \leq 16$. We integrate within the bounds $z_A = 1$ and $z_B = 16$. The boundary conditions applied are (30) at $z = z_A$, where as an approximation we take $F_p = F_M(v_1)$, and (29) at $z = z_B$. For T_p we take the upper estimate (38b). We remark that the solution of (20) and (21) was found to be insensitive to neglecting the $(1/z^2)$ term in the asymptotic boundary condition (29).

As a first case we take the nonlinear closure (22), corresponding to the perpendicular Maxwellian assumption (10). The result shown in Fig. 5 indicates good agreement with Fig. 1 in terms of the plateau values F_p and T_p. Next, in Fig. 6 we show the result

obtained with the linear closure (23). Again, although the solutions differ somewhat in detail, good general agreement with the 2-D result is obtained. It is of interest to note the result on the negative z-axis, shown in Fig. 6b (to be compared with the corresponding 2-D result on the negative $v_\parallel$-axis of Fig. 1). This is obtained by integrating (20) and (21), for negative z (where $D = 0$) starting at $z = -1$ with the same boundary conditions we took when integrating for positive z. Obviously then, the response we see is generated solely by the boundary conditions, which is how the fast particles pitch-angle scattered to positions below the plateau must be generated in the 1-D model.

One of the features of the fast particle population, evident from all our numerical results is the slow (compared with F_M) variation in z of their distribution function. This slowly varying distribution $\tilde{F}$ and the plateau height F_p can be calculated from the simplest approximation of the moment equations, obtained by imposing the closure (24) in Eq. (20) which then becomes

$$(Dz^3 + 1 + AT_p)\tilde{F}' + (A+1)z\tilde{F} = z^4 DF_M \,. \qquad (39)$$

The result of numerical integration shown in Fig. 7 is again in reasonable agreement with the 2-D result, but the principal advantage of this simple model is that it can be discussed analytically. Below the plateau we have

$$\tilde{F} = \tilde{F}_{hom}(z < v_1) = \tilde{F}_0 \exp(-\alpha_p z^2/2)\,;\ \alpha_p = \frac{A+1}{AT_p+1}\,, \qquad (40)$$

where $\tilde{F}_0 = \tilde{F}(0)$. Since $T_p > 1$, this distribution varies more slowly than F_M. On the plateau the distribution $\tilde{F}$ is made up of two contributions, the solution $\tilde{F}_{hom}$ of the homogeneous equation plus a particular integral F_s generated by the source term on the right hand side of Eq. (39). On the assumption that $Dv_1^3 \gg AT_p + 1$, we have

$$\tilde{F}_{hom}(z > v_1) \simeq C \exp\left[\frac{A+1}{D}\left(\frac{1}{z} - \frac{1}{v_1}\right)\right]\,, \qquad (41)$$

and

$$\tilde{F}_s = \exp\left(\frac{A+1}{Dz}\right) \int_{v_1}^{z} z' F_M(z') \exp\left(-\frac{A+1}{Dz'}\right) dz', \qquad (42)$$

where C is a constant to be determined from the condition of continuity of $\tilde{F}$ at the lower end of the plateau, $z = v_1$. Since $\tilde{F}_s(v_1) = 0$, we have $C = \tilde{F}_0 \exp(-\alpha_p v_1^2/2)$. The situation is sketched in Fig. 8. On the plateau we then have

$$\tilde{F}_p \approx \tilde{F}_0 \exp\left[-\alpha_p \frac{v_1^2}{2} + \frac{A+1}{D}\left(\frac{1}{z} - \frac{1}{v_1}\right)\right] + F_M(v_1) - F_M(z), \qquad (43)$$

where to evaluate the integral (42) we use the fact that for $D > 1$, $\exp[-(A+1)/Dz]$ changes much more slowly than $F_M(z)$. In sum then, neglecting the term in $1/D$, we obtain

$$F_p = \tilde{F}_p + F_M \simeq F_M(v_1) + \tilde{F}_0 \exp(-\alpha_p v_1^2/2). \qquad (44)$$

All that remains to be done is to determine $\tilde{F}_0$. We therefore recall our basic premise (based on 2-D results) that below the plateau, for small (i.e. bulk) values of $|z|$, where pitch-angle scattering is strong, the fast particle distribution function remains at approximately the plateau value F_p. We hence set $\tilde{F}_0 = F_p$ and obtain from (44)

$$F_p \simeq \frac{F_M(v_1)}{1 - \exp\left(-\alpha_p v_1^2/2\right)}, \qquad (45)$$

manifestly an increasing function of T_p, which itself is an increasing function of the plateau width and central phase velocity, as follows from (38). The plateau height thus estimated is in excellent agreement with the 2-D results of Table I.

We now examine the rf current density J and power density dissipated P_d. By definition,

$$J = \int_{-\infty}^{\infty} zF\, dz \qquad (46a)$$

$$P_d = \int_{-\infty}^{\infty} DzF'\, dz \qquad (46b)$$

15

whence we immediately get

$$J \approx F_p \left(\frac{v_2^2 - v_1^2}{2} \right) \qquad (47a)$$

$$P_d \approx F_p \frac{A+1}{3} \ln \left(\frac{Dv_2^3 + AT_p + 1}{Dv_1^3 + AT_p + 1} \right), \qquad (47b)$$

with the assumption that F on the plateau is almost constant, and taking for F'

$$F' \approx -F_p \frac{z(A+1)}{Dz^3 + AT_p + 1} \qquad (48)$$

obtained from (39) with $F = \tilde{F} + F_M$. The resulting J and P_d for four selected rf spectra are given in Table III. The current compares well with the 2-D result, but the estimated P_d are larger than their 2-D counterparts by factors of about three. Insofar as the 1-D approximation for F compares well with the 2-D result (cf. Table I) an agreement between the two currents is to be expected. The discrepancy in P_d then can only be explained on the basis that the slope F'/F_p given by (48) is too large. In order to understand this shortcoming of the approximation (48) we recall that the averaged flux (16) [which gives (48) upon substituting $F_2 = 2T_pF$] was derived by setting $v \to v_\parallel$ in integrals of the type (see Appendix)

$$g_n^{(m)} = \int_0^\infty v^{-m} v_\perp^{n+1} f \, dv_\perp \qquad (49)$$

and is therefore a valid approximation only for $v_\parallel^2 \gg 2T_p$. However, this condition is not satisfied everywhere within the velocity bounds of current drive spectra, and so the integrals $g_n^{(m)}$, are overestimated. A better approximation of the $g_n^{(m)}$ (see the Appendix for details) yields

$$F' = -F \frac{z[(A/a_1) + B(1 - 2/z^2 a_5)]}{Da_3z^3 + (AT_p/a_1) + (Ba_3/a_5)} \qquad (50)$$

16

where $a_m = 1 + mT_p/z^2$. The resulting J/P_d given in Table III now agree very well with the 2-D results. We emphasize that for relatively flat plateaus the figure of merit J/P_d is almost independent of the plateau height F_p. For large $T_p \gg 1$ we can ignore the last terms in the numerator and denominator of (50) and thus obtain the simple result (in units of $e/m\nu_0 v_e$)

$$\frac{J}{P_d} \approx \frac{(v_2^2 - v_1^2)}{2D} \left[\int_{v_1}^{v_2} \frac{z^2(A + Ba_1)}{Da_1a_3z^3 + AT_p} \, dz \right]^{-1} \tag{51}$$

In conclusion, we have derived a 1-D representation of the 2-D Fokker-Planck equation for lower-hybrid current drive, namely Eqs. (20) and (21), which, when taken together with one of the closure assumptions, (22) or (23) or (24), describe the evolution in $v_\parallel$ of the first two perpendicular moments (7) of the distribution function. The method is based on the assumption, supported by 2-D numerical results, that the departures of the distribution function from the thermal (i.e. bulk) Maxwellian equilibrium (caused by the fast particles generated in the region of the rf spectrum) take the form of a distribution broadened in the perpendicular direction. The first closure condition (22) is based upon assuming that the distribution function (12) of fast particles $\tilde{f}$ is of Maxwellian form (10); this results in Eqs. (20) and (21) being nonlinear. The second, alternate closure condition (23) does not assume a specific form for $\tilde{f}$ but requires an estimate of the plateau temperature T_p which we provide through (37); this results in Eqs. (20) and (21) being linear. Finally, the third, alternate closure (24), with (37), leads to the simplest 1-D model of a single linear differential equation. Our results clearly show that either the first alternate closure (22) or the second alternate closure (23), together with (37) for T_p, give the best reproduction of the 2-D numerical results; both the height of the plateau, which determines the current generated, and the perpendicular temperature, as a function of $v_\parallel$, are well reproduced. The advantage of the second alternate closure is that it does not assume a particular form for $\tilde{f}$, and that it leads to a linear system

which is much simpler to solve. Even the simplest closure (24), together with (37), which leads to only one linear equation, gives the correct plateau height and current while the perpendicular temperature is just the satisfactory estimate from (37) (see Table II). The power dissipated requires a very accurate estimate of F' on the plateau and is calculated on the basis of (50). The figure of merit J/P_d is then given by (51). This then achieves a more predictive formulation of LH current drive in 1-D.

ACKNOWLEDGMENTS

APPENDIX

PERPENDICULAR-VELOCITY AVERAGING OF THE FOKKER-PLANCK EQUATION

Our 1-D approximation of the steady-state 2-D Fokker-Planck equation

$$\text{div}\vec{S} = \frac{\partial S_\parallel}{\partial v_\parallel} + \frac{1}{v_\perp}\frac{\partial}{\partial v_\perp}(v_\perp S_\perp) = 0 \,, \tag{A1}$$

where

$$S_\parallel = -Bf\frac{v_\parallel}{v^3} - \frac{\partial f}{\partial v_\parallel}\left(D + \frac{A}{2}\frac{v_\perp^2}{v^3} + B\frac{v_\parallel^2}{v^5}\right) + \frac{\partial f}{\partial v_\perp}\frac{v_\perp v_\parallel}{v^3}\left(\frac{A}{2} - \frac{B}{v^2}\right) \tag{A2}$$

and

$$S_\perp = -Bf\frac{v_\perp}{v^3} + \frac{\partial f}{\partial v_\parallel}\frac{v_\perp v_\parallel}{v^3}\left(\frac{A}{2} - \frac{B}{v^2}\right) - \frac{\partial f}{\partial v_\perp}\frac{1}{v^3}\left(\frac{A}{2}v_\parallel^2 + B\frac{v_\perp^2}{v^2}\right) \,, \tag{A3}$$

is based on the two perpendicular-velocity moments of (A1):

$$2\pi\int_0^\infty v_\perp^{n+1}\,\text{div}\vec{S}\,dv_\perp \,; \quad n = 0, 2, \ldots . \tag{A4}$$

This immediately gives for $n = 0$

$$S_0' = 0 \tag{A5}$$

and for $n = 2$

$$S_2' - 4\pi\int_0^\infty v_\perp^2 S_\perp\,dv_\perp = 0 \,, \tag{A6}$$

where we define

$$S_n = 2\pi\int_0^\infty v_\perp^{n+1}S_\parallel\,dv_\perp \,, \tag{A7}$$

and the prime stands for the derivative with respect to $v_\parallel$. The explicit form of Eqs. (A5) and (A6) depends upon integrals of the type

$$g_n^{(m)} = \int_0^\infty v^{-m}v_\perp^{n+1}f\,dv_\perp \,. \tag{A8}$$

19

We begin with a simple approximation of $g_n^{(m)}$, based upon the assumption that the particles of interest, i.e. those populating the resonant region, have $v_\parallel \gg v_\perp$. We thus set $v \to v_\parallel$, giving

$$g_n^{(m)} \simeq F_n / 2\pi v_\parallel^m \,, \qquad (A9)$$

where F_n is the n-th moment of the distribution function f, i.e.

$$F_n = 2\pi \int_0^\infty v_\perp^{n+1} f \, dv_\perp \,. \qquad (A10)$$

The integrations in (A5) and (A6) are then carried out in a straightforward manner, first integrating by parts the expression depending on $\partial f / \partial v_\perp$. We thus obtain

$$S_0 = -\left(D + \frac{B}{v_\parallel^3}\right)F_0' - \frac{A+B}{v_\parallel^2}F_0 - \frac{A}{2v_\parallel^3}F_2' + \frac{2B}{v_\parallel^4}F_0 \,, \qquad (A11)$$

$$S_2 = -\left(D + \frac{B}{v_\parallel^3}\right)F_2' - \frac{2A+B}{v_\parallel^2}F_2 - \frac{A}{2v_\parallel^3}F_4' + \frac{4B}{v_\parallel^4}F_2 \,, \qquad (A12)$$

and

$$4\pi \int_0^\infty v_\perp^2 S_\perp \, dv_\perp = \frac{2AF_0}{v_\parallel} + \frac{AF_2'}{v_\parallel^2} - \frac{2BF_2}{v_\parallel^3} - \frac{2BF_2'}{v_\parallel^4} + \frac{8BF_2}{v_\parallel^5} \,. \qquad (A13)$$

Since for resonant electrons $v_\parallel$ is much larger than the thermal velocity, i.e. $v_\parallel \gg 1$, we can neglect the last terms in these three equations. The expressions (A11) through (A13) are then asymptotically correct in $v_\parallel$ since they identically vanish for the equilibrium distribution function

$$f_M = (2\pi)^{-3/2} \exp(-v^2/2), \qquad (A14)$$

which is the solution of (A1) when $D = 0$. In this context, we note that for Gaussians of the type (10) the moments F_n are simply

$$F_n = \frac{F}{T_\perp} \frac{1}{2} (2T_\perp)^{\frac{n}{2}+'} \Gamma(\frac{n}{2}+1), \qquad (A15)$$

so that $F_{n+2} = (n+2)T_\perp F_n$. In equilibrium, of course, $T_\perp = 1$. Realizing further that there is also no need to retain in Eq. (A13) the term $2BF_2'/v_{\parallel}^4$, Eqs. (A11-13) then give Eqs. (16), (18) and (19) used in Sec. III.

We will now discuss the conditions of validity of the given model in the resonant region. Our discussion will be based on the fast particle distribution function (10), for which the integrals (A8) can be written in the form

$$g_n^{(m)} = I_n^{(m)} F / 2\pi T_p, \qquad (A16)$$

where

$$I_n^{(m)} = \int_0^\infty v^{-m} v_\perp^{n+1} \exp(-v_\perp^2/2T_p) \, dv_\perp, \qquad (A17)$$

and T_p is the perpendicular temperature in the resonant region. Changing variables first from $v_\perp$ to v and subsequently from v^2 to $2T_p u$ gives

$$I_n^{(m)} = T_p (2T_p)^{-m/2} e^q \int_q^\infty u^{-m/2} e^{-u} (2T_p u - v_{\parallel}^2)^{n/2} \, du \qquad (A18)$$

where $q = v_{\parallel}^2/2T_p$. We only need to consider $n = 0, 2$ and 4, and for these we get

$$I_0^{(m)} = T_p (2T_p)^{-m/2} e^q \, \gamma(1 - m/2, q), \qquad (A19)$$

$$I_2^{(m)} = -v_{\parallel}^2 I_0^{(m)} + 2T_p^2 (2T_p)^{-m/2} e^q \, \gamma(2 - m/2, q), \qquad (A20)$$

and

$$I_4^{(m)} = -v_{\parallel}^4 I_0^{(m)} - 2v_{\parallel}^2 I_2^{(m)} + 4T_p^3 (2T_p)^{-m/2} e^q \, \gamma(3 - m/2, q), \qquad (A21)$$

where $\gamma(\alpha, q)$ is the incomplete gamma function[7]

$$\gamma(\alpha, q) = \int_q^\infty t^{\alpha-1} e^{-t} \, dt. \qquad (A22)$$

Electrons in the resonant region typically have $v_\parallel^2 \gg 1$, and if also $v_\parallel^2/2T_p$ is sufficiently large, i.e. $v_\parallel^2/2T_p > 1$, then $\gamma(\alpha, q)$ can be very well approximated by suitably truncating its continued fraction expansion[7]

$$\gamma(\alpha, q) = \cfrac{e^{-q}q^\alpha}{q + \cfrac{1-\alpha}{1 + \cfrac{1}{q + \cfrac{2-\alpha}{1 + \cfrac{2}{q + \cfrac{3-a}{1+\ldots}}}}}} \qquad (A23)$$

To lowest order this gives $e^{-q}q^{\alpha-1}$, which is just the leading term of the large-q asymptotic expansion of $\gamma(\alpha, q)$. To this order $I_2^{(m)}$ and $I_4^{(m)}$ vanish, so that we have to go to the next order, which is

$$\gamma(\alpha, q) \sim \frac{e^{-q}q^\alpha}{q + 1 - \alpha}. \qquad (A24)$$

We have verified that as long as $q + 1 - \alpha > 0$, this last approximation is excellent even when $q \to 1$, for which the asymptotic expansion for γ breaks down completely.

Upon substituting (A24) into (A19) through (A21) we obtain, after some algebra,

$$I_0^{(m)} = \frac{T_p}{v_\parallel^m} \frac{1}{a_m} \qquad (A25)$$

$$I_2^{(m)} = \frac{2T_p^2}{v_\parallel^m} \frac{1}{a_m} \frac{1}{a_{m-2}} \qquad (A26)$$

$$I_4^{(m)} = \frac{8T_p^3}{v_\parallel^m} \frac{1}{a_m} \frac{1}{a_{m-2}} \frac{1}{a_{m-4}}, \qquad (A27)$$

where

$$a_m = 1 + m/2q = 1 + m\frac{T_p}{v_\parallel^2}. \qquad (A28)$$

For large $q \gg 1$, such that we can take $a_m \simeq 1$, we now immediately recover the result (A9), where for F_n the expression (A15) is substituted. We thus conclude that the approximation (A9) is valid when $v_\parallel^2 / 2 T_p \gg 1$. Qualitatively, this can be understood on the basis that particles having $v_\perp$ larger than the perpendicular width $\sqrt{2 T_p}$ of the distribution function do not contribute to $g_n^{(m)}$. Therefore, if $(v_\parallel^2 / 2 T_p) \gg 1$ then v^2 can be replaced by $v_\parallel^2$.

We now relax the condition $v_\parallel^2 / 2 T_p \gg 1$, so that spectra can be considered having a lower boundary v_1 around $v_\parallel = 4$, and producing high T_p such as we see in Table II. On the plateau we assume that T_p is constant and given by Eq. (37). Then only the moment $F_0 \equiv F$ is unknown, and is given by Eq. (A5) where $F_2 = 2 T_p F$ is substituted. Since the net particle flux vanishes, the integration constant in (A5) is zero and the equation becomes $S_0 = 0$. In terms of the $I_n^{(m)}$ we get

$$
F' \left[D + \frac{1}{T_p} \left(\frac{A}{2} I_2^{(3)} + B v_\parallel^2 I_0^{(5)} \right) \right] + \frac{F}{T_p^2} \left(\frac{A}{2} v_\parallel I_2^{(3)} - B v_\parallel I_2^{(5)} + B v_\parallel T_p I_0^{(3)} \right) = 0 , \qquad (A28)
$$

which, upon substituting $I_n^{(m)}$ from (A25) through (A27), gives Eq. (50) of the main text.

REFERENCES

1. N. J. Fisch, *Phys. Rev. Lett.* <u>41</u>, 873 (1978).

2. D. Hewett, K. Hizanidis, V. Krapchev and A. Bers, *Proc. IAEA Tech. Comm. Meeting on Non-Inductive Current Drive in Tokamaks*, edited by D. F. H. Start (Culham Laboratory, Abingdon, Oxon, U.K., 1983) Culham Laboratory Report CLM-CD (1983), Vol. I. p. 124.

3. K. Hizanidis, V. Krapchev and A. Bers, *Proceedings of the Fifth Topical Conference on RF Plasma Heating*, University of Wisconsin-Madison, Madison, Wisconsin, 21-23 February 1983, pp. 160–163.

4. *TWODEPEP, IMSL Problem-Solving Software System for Partial Differential Equations* (IMSL, Houston, Texas, 1983), IMSL Report TDP-0005, Edition 5.

5. R. M. Kulsrud, Y. C. Sun, N. K. Winsor, and H. A. Fallon, *Phys. Rev. Lett.* <u>31</u>, 690 (1973).

6. B. A. Trubnikov, *Reviews of Plasma Physics*, edited by M. A. Leontovich (Consultants Bureau, New York, 1965), Vol. 1, p. 105.

7. I. S. Gradshteyn and I. M. Ryzhik, <u>Table of Integrals, Series, and Products</u>, Academic Press, New York (1980), pp. 940-942.

FIGURE CAPTIONS

Fig. 1   Results from a 2-D numerical integration of Eqs. (2)–(5). The parallel distribution function $F = F_0$ and the perpendicular temperature $T_\perp = F_2/2F_0$ as a function of $v_\parallel \equiv z$ for $D = 3$ within the bounds $v_1 \leq v_\parallel \leq v_2$, and $D = 0$ elsewhere.

Fig. 2   Characteristics of the 2-D particle flux in velocity space. (a) Results from a 2-D numerical integration of Eqs. (2)–(5). Orientation of the particle flux vector $\vec{S}$ in the $(v_\parallel, v_\perp)$ plane. (b) Schematic representation of particle flow into and out of the resonant region.

Fig. 3   Results from a 2-D numerical integration of Eqs. (2)–(5). Perpendicular velocity moments of $\tilde{f} = f - f_M$ as a function of $v_\parallel$.

Fig. 4   Results from a 2-D numerical integration of Eqs. (2)–(5). Cuts of the distribution function f taken at six different positions of $v_\parallel$, as a function of $v_\perp^2$.

Fig. 5   1-D result: the distribution function $F = F_0$ and the perpendicular temperature $T_\perp = F_2/2F_0$ as a function of $v_\parallel$, calculated from Eqs. (20) and (21) with the closure (22).

Fig. 6   As in Fig. 5 but with the closure (23). (a) $v_\parallel > 0$. (b) $v_\parallel < 0$.

Fig. 7   As in Fig. 5 but calculated from Eq. (20), with the closure (24).

Fig. 8   The slowly varying distribution function $\tilde{F}$ and its matching to the plateau.

TABLE CAPTIONS

TABLE I – The perpendicular temperature T_p [defined by (7) and (8)] of the plateau particles, and the plateau height F_p, as functions of rf spectrum location.

TABLE II – Plateau temperatures. The minimum, $T_p(\min)$, and the maximum, $T_p(\max)$, estimated values [from Eqs. (37) and (38)], and the corresponding 2-D result.

TABLE III – Rf current density J, power density dissipated, P_d, and figure of merit J/P_d. Comparison of 2-D numerical results with 1-D approximations. For all cases $D = 3$.

FIG. 1

27

$$\frac{D=3}{v_1=4, \; v_2=12}$$

Fast

Fast particles out

Thermal particles in

Maxwellian bulk

Plateau region

v_1 v_2

FIG. 2

28

FIG. 3

FIG. 4

30

FIG. 5

FIG.6a

FIG. 6b

FIG. 7

34

$\tilde{F}$

$\tilde{F}_{hom}$

$\tilde{F}_p$

$\tilde{F}_0$

$\tilde{F}_{hom}$

$\tilde{F}_s$
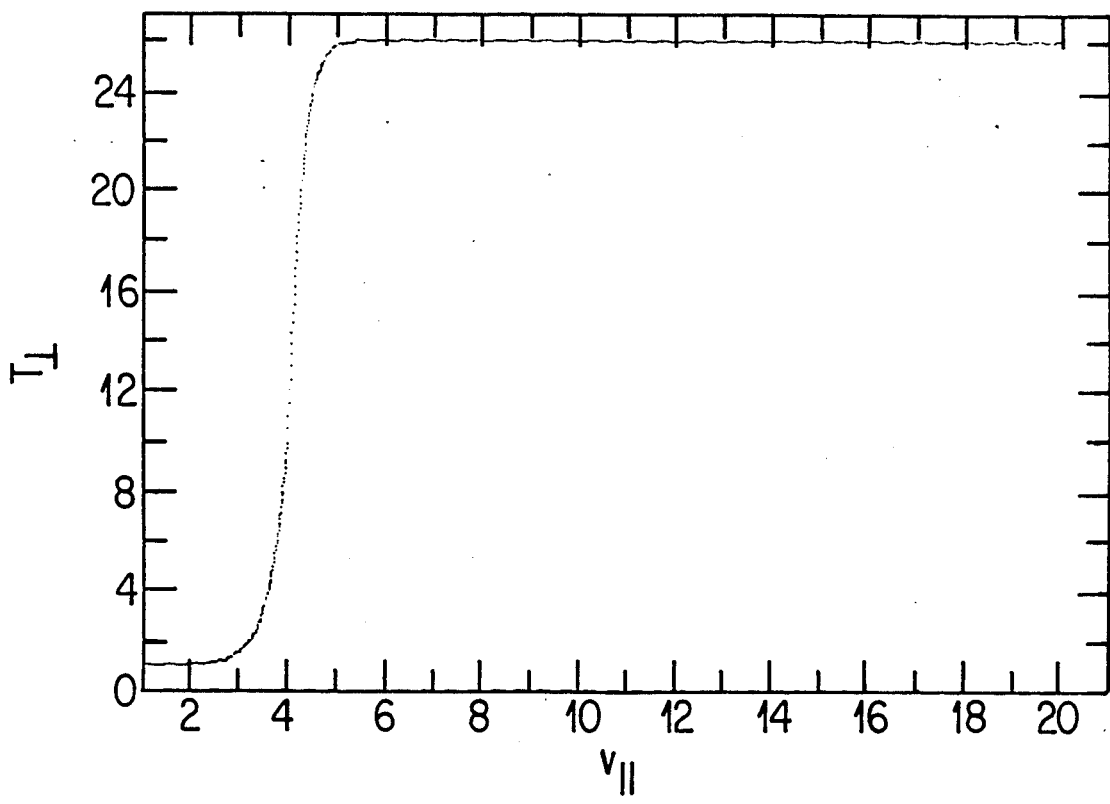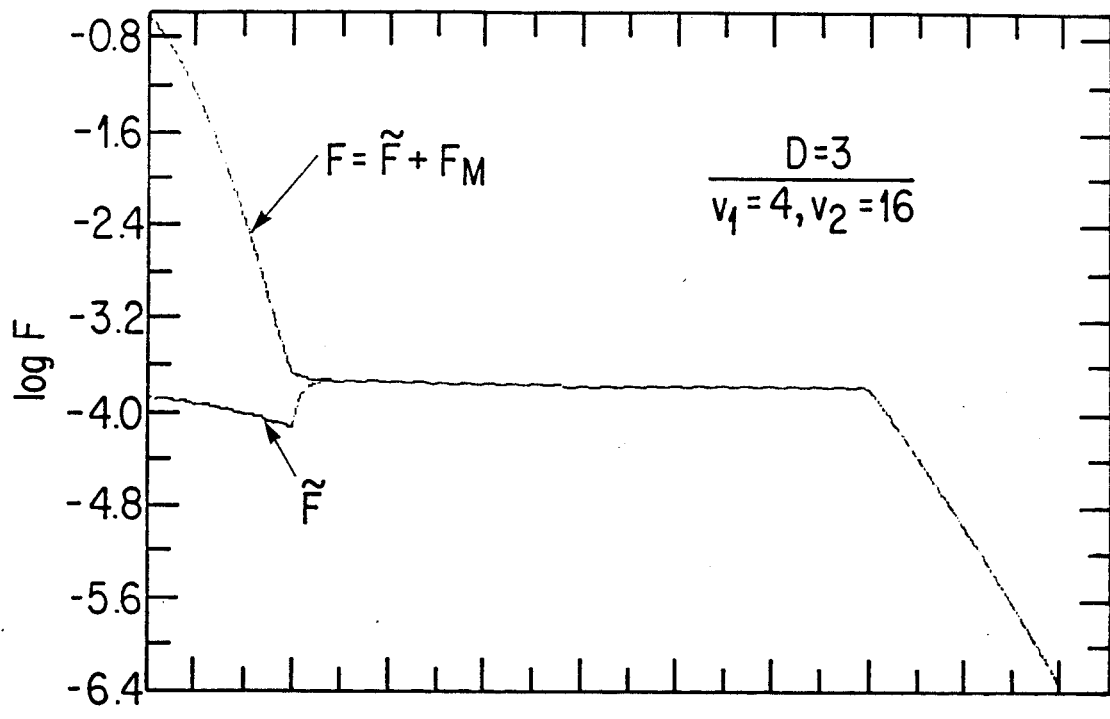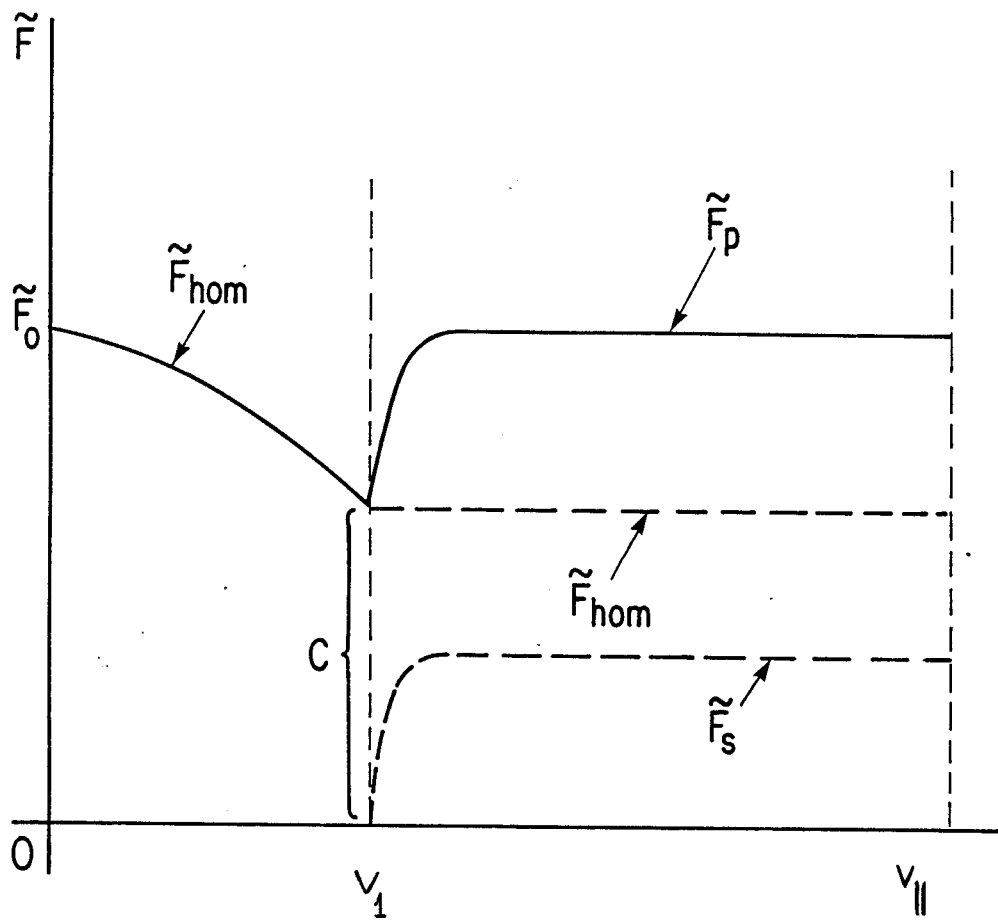
C

0

V_1

$V_{\parallel}$
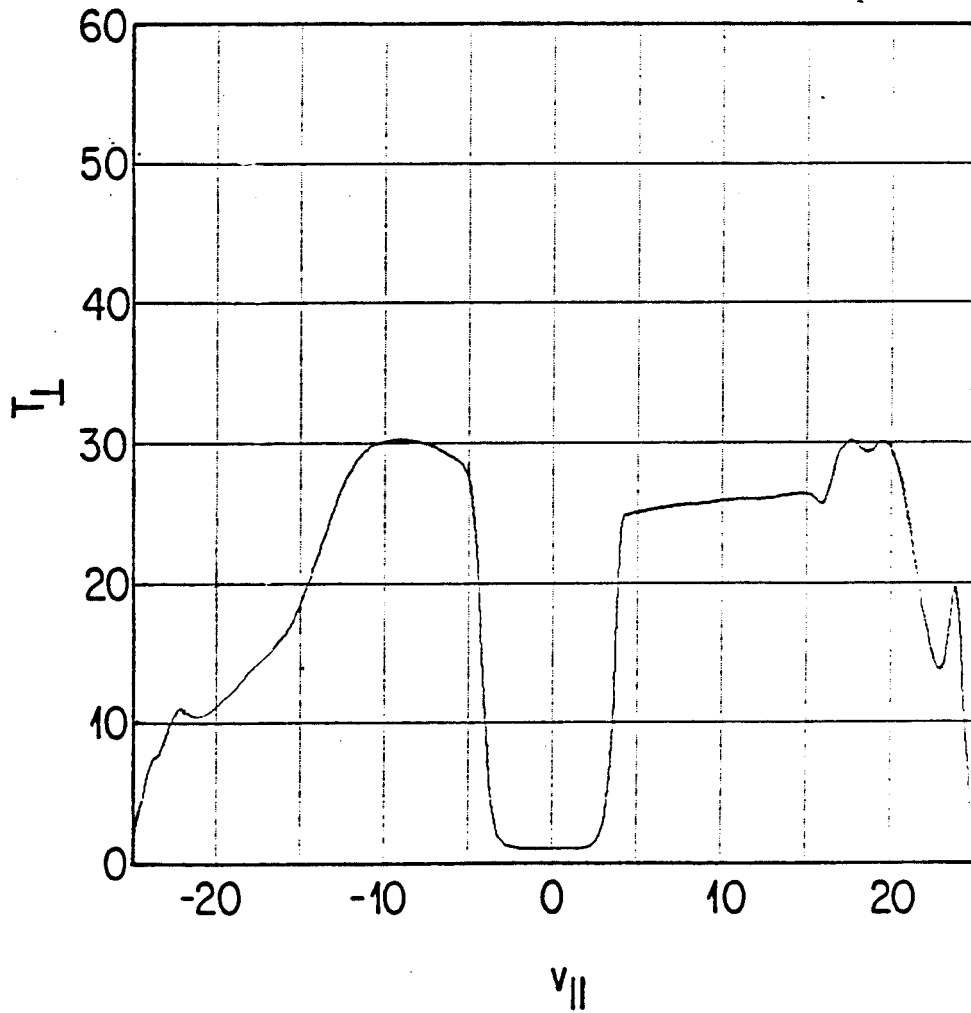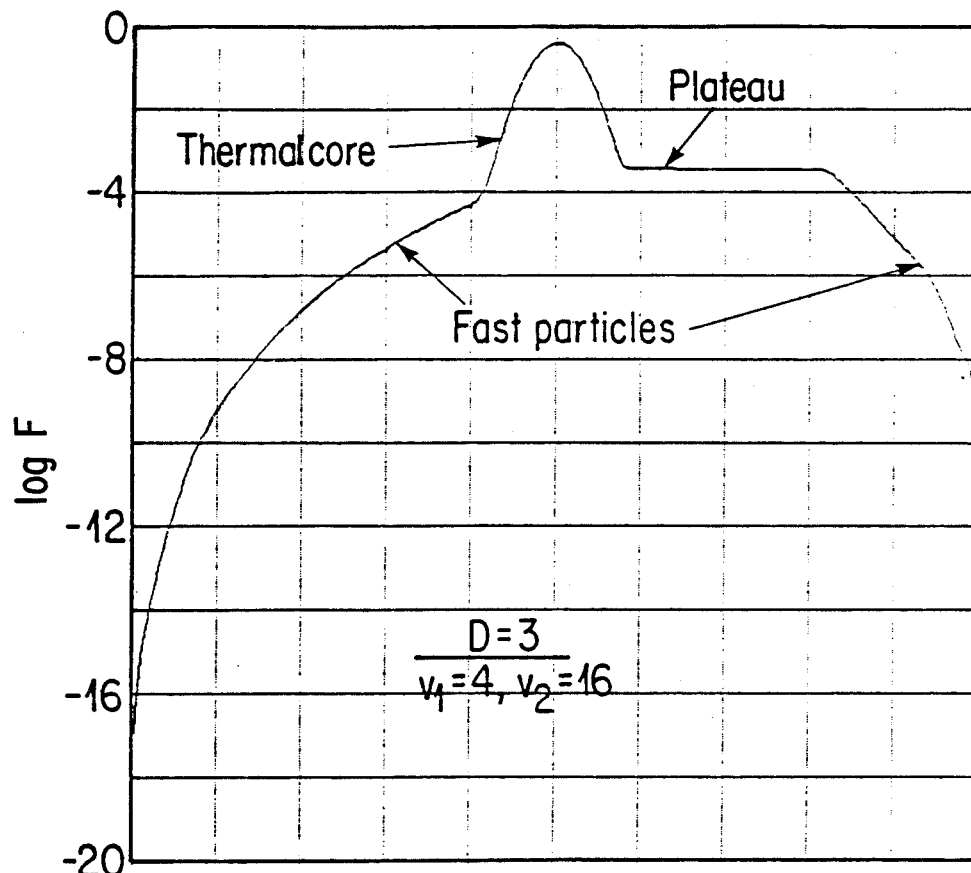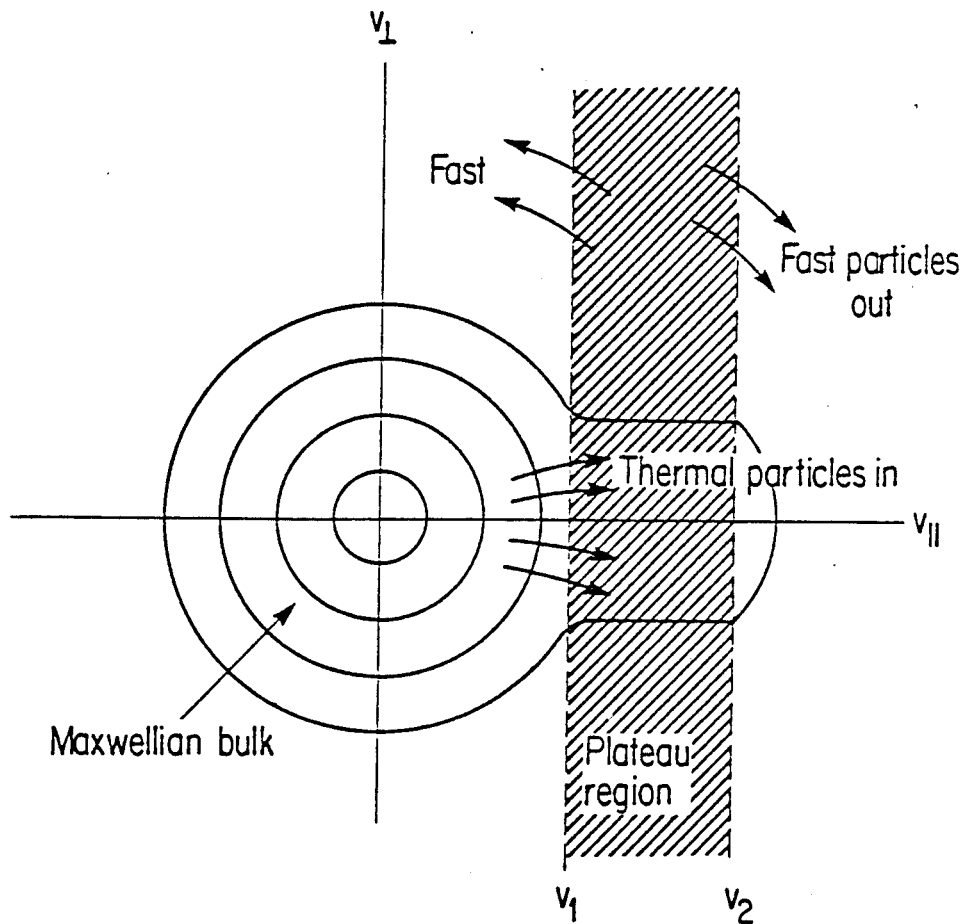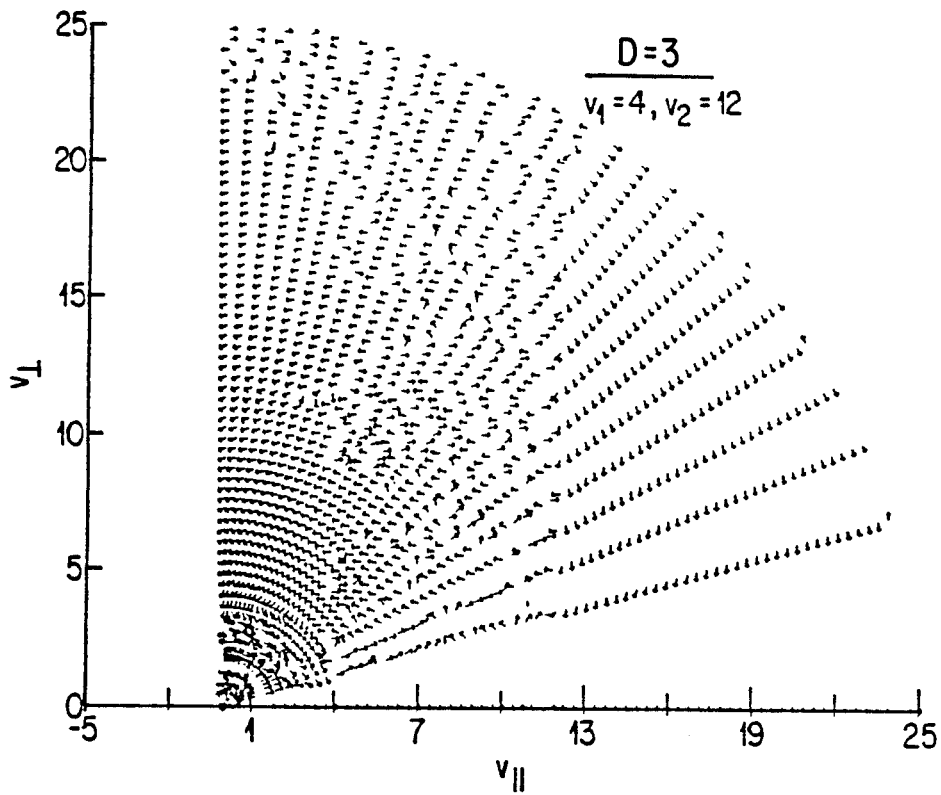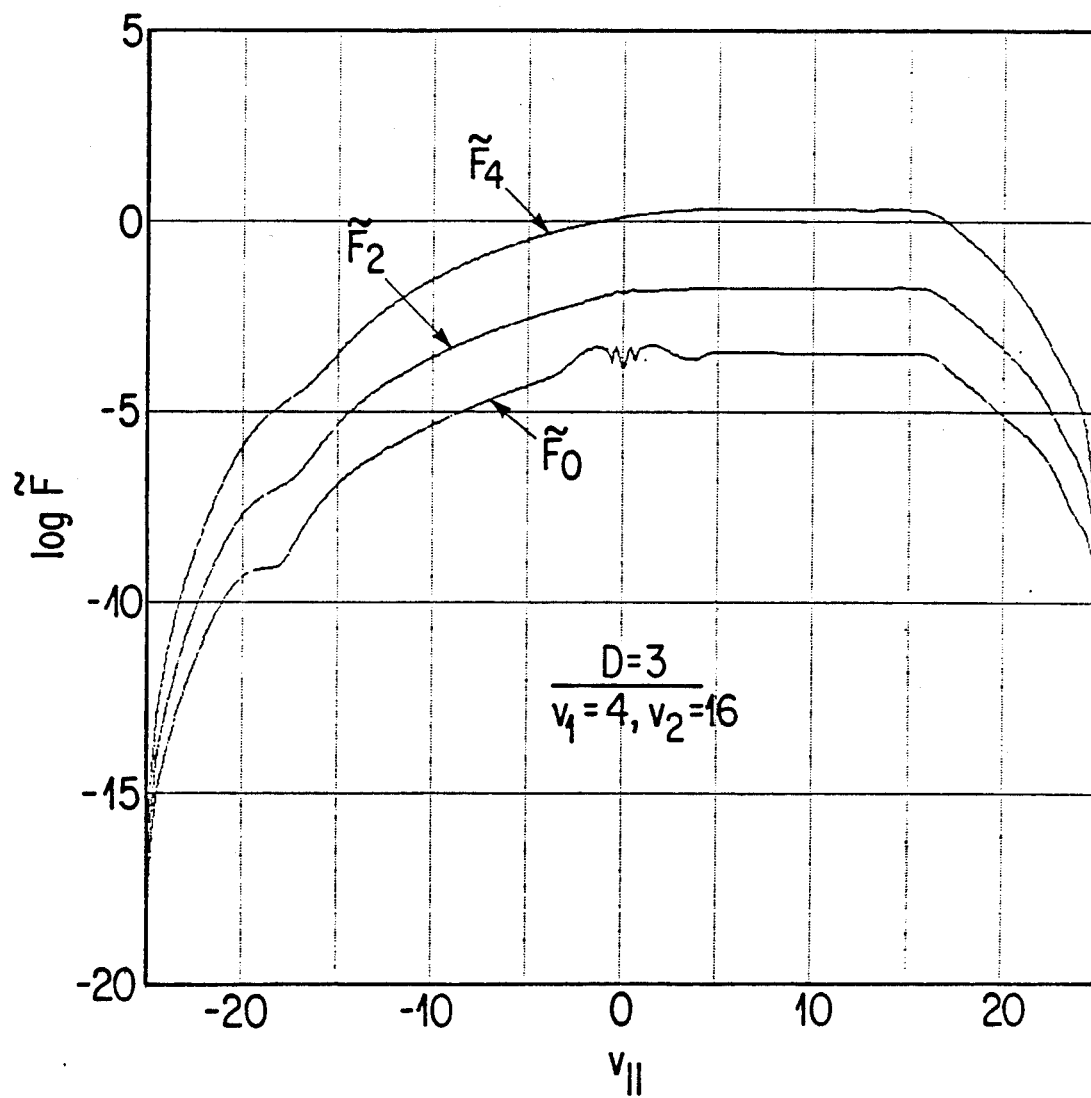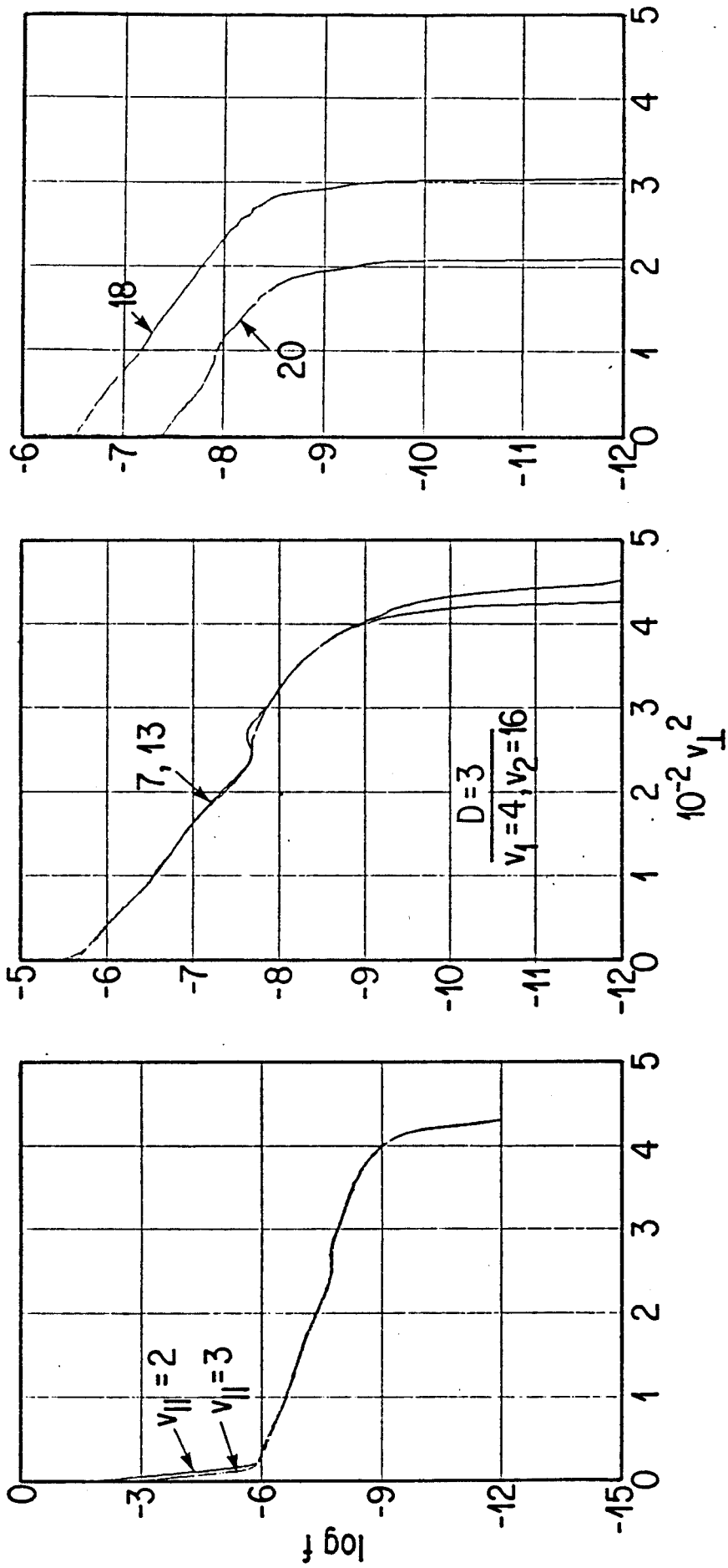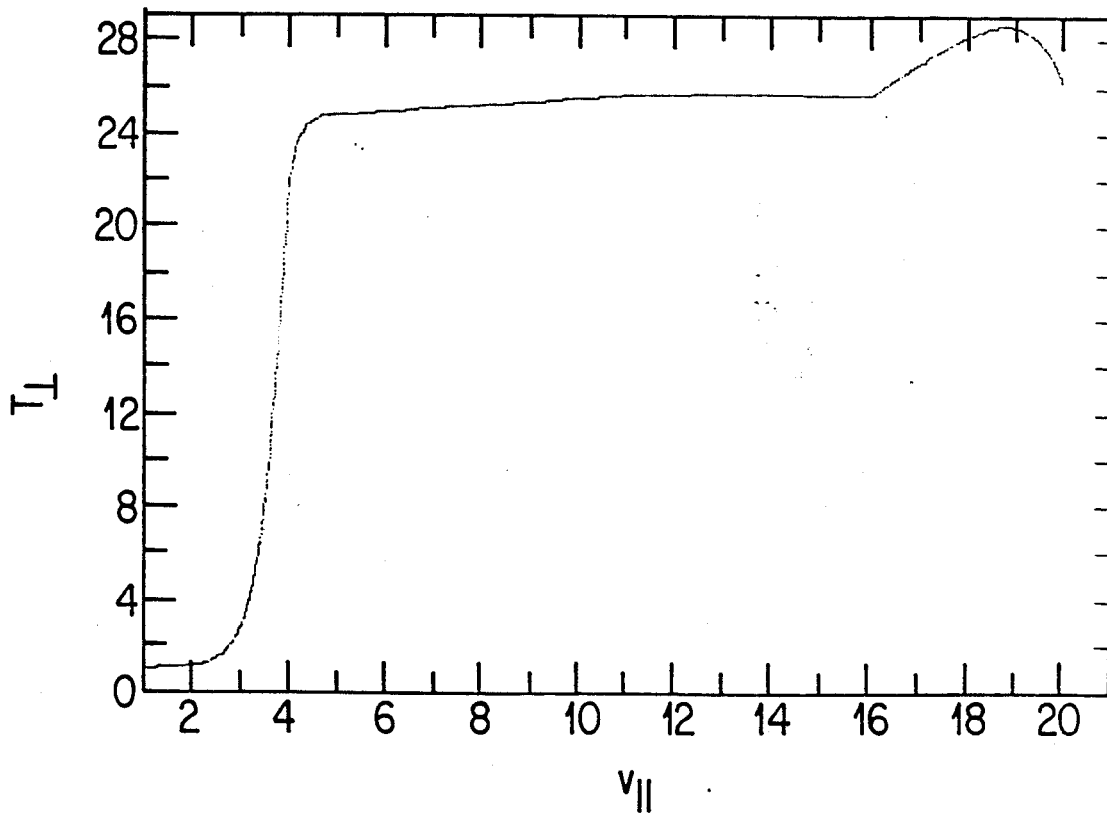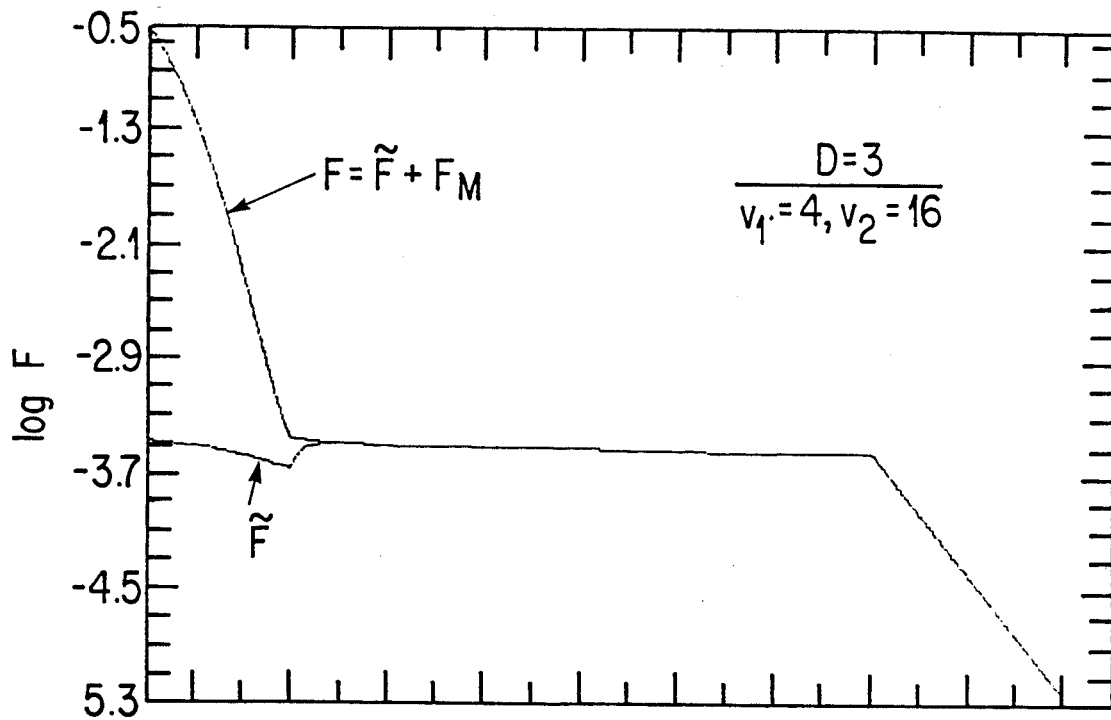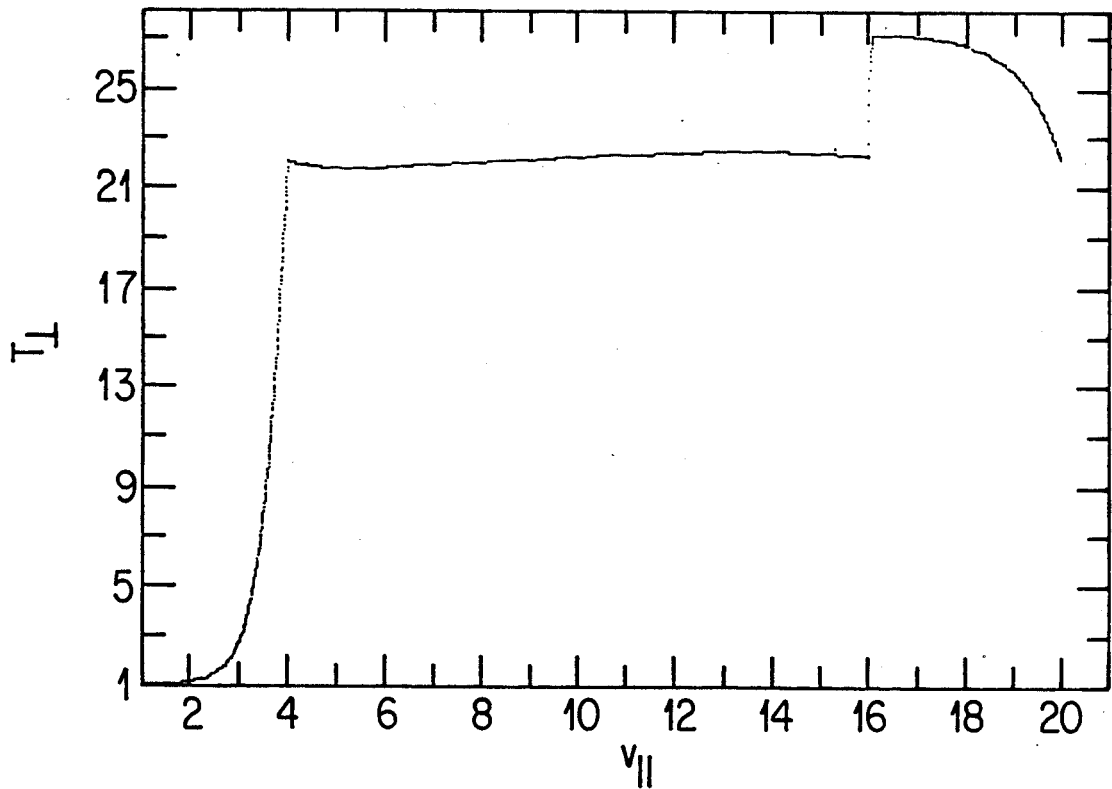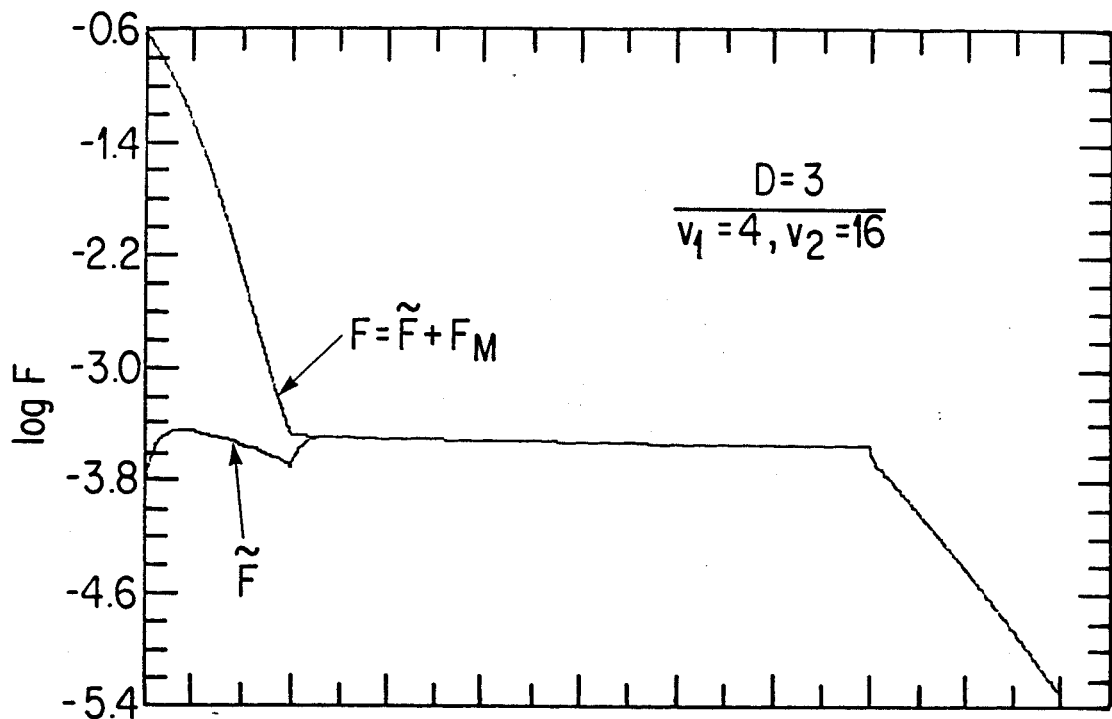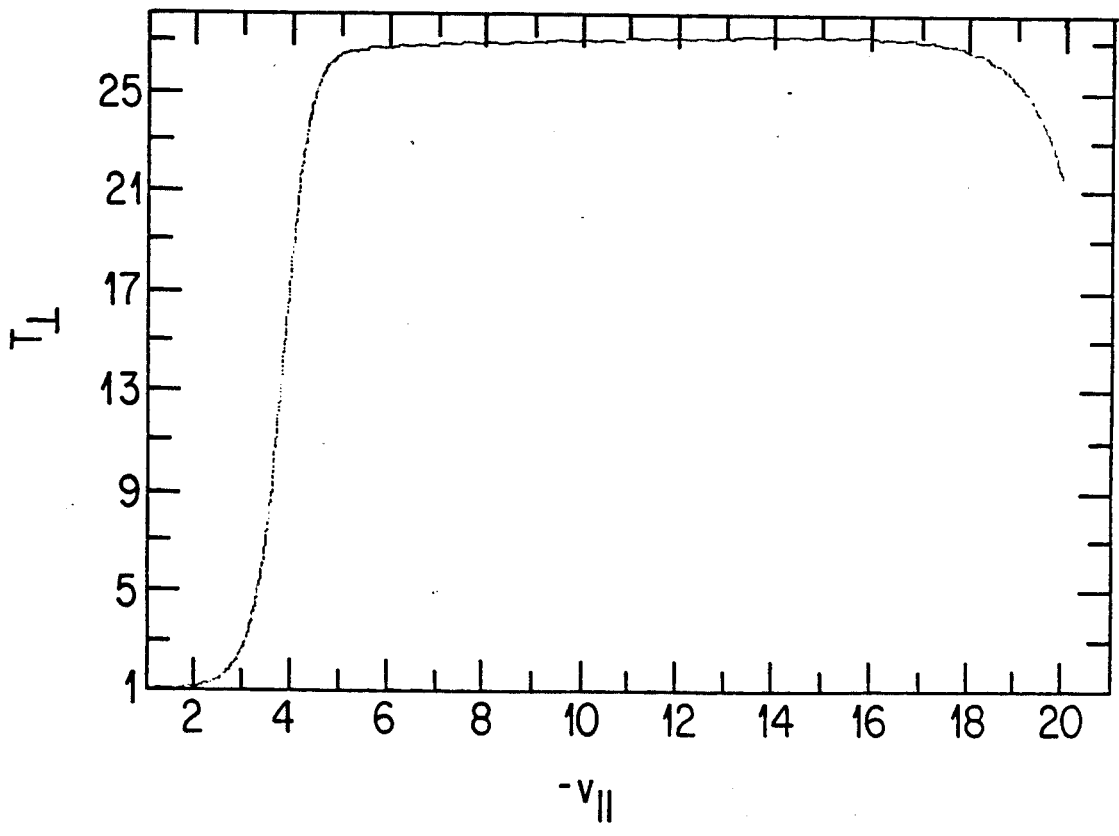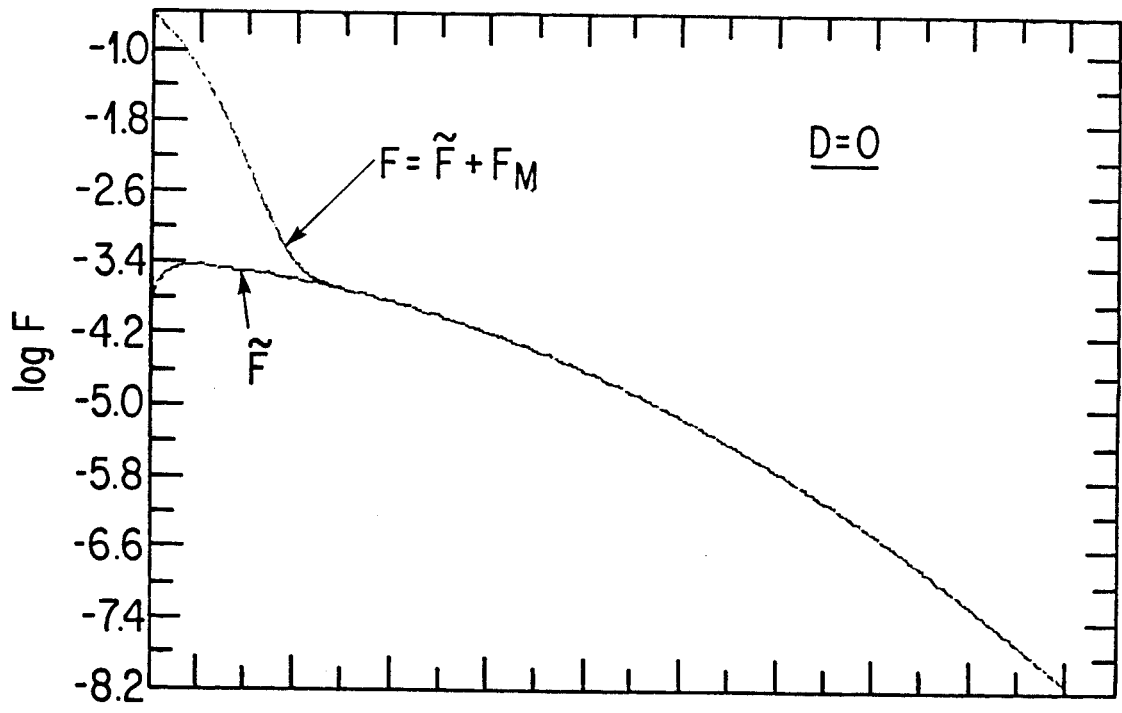
FIG. 8

TABLE I

Spectrum limits $[v_1, v_2]$	Ion charge number Z_i	T_p from (2 - D) numerical	$F_p \times 10^4$ from (2 - D) numerical	$F_p \times 10^4$ Eq. (45)
[4,8]	1	9	2.4	1.86
[4,12]	1	17	3.0	2.70
[4,16]	1	26	3.5	3.67
[4,16]	4	43	5.5	6.67
[4,16]	9	53	7.5	8.6
[4,20]	1	33	4.5	4.45

TABLE II

Spectrum limits $[v_1, v_2]$	Ion charge number Z_i	T_p from (2 - D) numerical	$T_p(min)$ Eqs. (37),(38a)	$T_p(max)$ Eqs. (37),(38b)
[3,5]	1	4	2	3.7
[4,8]	1	9	6	9.6
[4,12]	1	17	13	20
[4,16]	1	26	20	29
[4,16]	4	43	32	47
[4,16]	9	53	39	60
[4,20]	1	33	28	38

TABLE III

Spectrum limits $[v_1, v_2]$	Ion charge number Z_i	2D, Numerical			1D, Analytic Eqs. (45),(47a,b)			1D, Analytic Eqs.(47a),(51)	
		$10^2 J$	$10^5 P_d$	J/P_d	$10^2 J$	$10^5 P_d$	J/P_d	$10^5 P_d$	J/P_d
[4,8]	1	.70	24	29	0.44	37	12	17	26
[4,12]	1	2.3	43	53	1.72	108	16	36	48
[4,16]	1	4.8	63	77	4.4	144	31	58	76
[4,16]	4	7.3	134	55	8.0	457	18	138	58
[4,16]	9	9.2	270	34	10	906	11	264	38
[4,20]	1	10	93	108	8.5	202	42	82	104